

Received February 11, 2019, accepted March 1, 2019, date of publication April 19, 2019, date of current version April 26, 2019.

Digital Object Identifier 10.1109/ACCESS.2019.2904613

# Joint DOD and DOA Estimation in Bistatic MIMO Radar With Distributed Nested Arrays

YANPING LIAO<sup>1</sup>, RUIGANG ZHAO<sup>1</sup>, AND LIPENG GAO<sup>1</sup>

Department of Information and Communication Engineering, Harbin Engineering University, Harbin 150001, China

Corresponding author: Lipeng Gao (gaolipeng@hrbeu.edu.cn)

This work was supported in part by the National Key Research and Development Program of China under Grant 2016YFC0101700, in part by the National Nature Science of Foundation of China under Grant 61301201 and Grant 61371175, and in part by the Heilongjiang Postdoctoral Research Foundation under Grant LBH-Q14039.

**ABSTRACT** In this paper, we investigate the problem of joint direction of departure (DOD) and the direction of arrival (DOA) estimation in bistatic MIMO radar. A new bistatic MIMO radar with the distributed nested array is proposed. Based on the new array, the DOD and DOA estimation algorithm called automatically paired DR-ESPRIT based on the angle disambiguation algorithm by using the range information of targets is proposed. By designing distributed nested array and using Khatri-Rao product processing, the long baseline and short baseline in the transceiver arrays are virtually extended simultaneously. The non-ambiguous and high-accuracy sine estimations of the DOD and DOA can be accomplished using DR-ESPRIT algorithm and the range information of targets and the geometry of bistatic MIMO radar. The virtual extension of array aperture and high angle estimation accuracy can be achieved for the MIMO radar with automatic pairing and without increasing the number of antennas compared with traditional uniform linear MIMO array. And, the proposed corresponding algorithm gives significant improvement in the DOD and DOA estimation performance. The simulation results validate the theoretical algorithm.

**INDEX TERMS** Bistatic MIMO radar, distributed nested array, DOD and DOA estimation, disambiguation, DR-ESPRIT.

## I. INTRODUCTION

Multiple-input multiple-output (MIMO) radar which refers to radar systems with multiple antennas to transmit diverse waveforms and multiple antennas to receive targets echoes, has shown enhanced capability compared with its phased array counterpart [1]–[2]. Compared with the traditional radar, it has advantages in anti-stealth, anti-jamming, freedom of freedom, angle resolution and angle measurement precision [3]–[4]. It has attracted more and more attention owing to its significant performance improvement in target detection, parameter estimation, clutter suppression compared with the conventional phased-array radar. Specifically, the problem of joint estimation of the direction-of-departure (DOD) and direction-of-arrival (DOA) is widely investigated. Some methods have been proposed [5]–[9]. The reduced-dimensional Capon (RD-Capon) [5] and reduced-dimensional multiple signal classification (RD-MUSIC) algorithms [6] are presented to jointly estimate the DOD

and DOA. But the high computational cost is employed due to the two-dimensional angle searching. And the ESPRIT methods [7]–[8] are developed. But an additional pair matching between DOD and DOA estimation is required. Another automatic pairing procedure, called combined ESPRIT-Root-MUSIC algorithm, which uses the ESPRIT method to estimate the DOD and the Root-MUSIC for the DOA estimation is proposed in [9]. But the constraint conditions lead to some loss of angle estimation performance owing to the inadequate utilization of received data. Therefore, the non-uniform array is introduced into the MIMO radar signal processing in order to get the larger array aperture without increasing the number of sensors. The idea of minimal redundancy is applied to array optimization design of MIMO radar in [10]. The DOA estimation configuring minimum redundant array in both the transmit array and receive array has been addressed in [11]. But the computational complexity is higher because the minimum redundant array element position requires exhaustive searching. The joint estimation of DOD and DOA based on the coprime arrays and the nested arrays is presented in [12] and [13] by utilizing the MUSIC algorithm and spatial

The associate editor coordinating the review of this manuscript and approving it for publication was Salman Ahmed.

smoothing technique. However, the angle estimation accuracy of [12] and [13] has not been improved at all.

It is well known that the angle estimation accuracy is critically dependent on the array aperture. The distributed array can provide very accurate estimation without extra antennas [14]–[15]. Thus, link bistatic MIMO radar to separated subarray, the bistatic MIMO radar system which both transmit array and receive array consist of sparse linear subarrays is proposed in [16]. Then the new joint DOD and DOA estimation algorithm, called ESPRIT-MUSIC algorithm and Reduced-Dimension ESPRIT-MUSIC algorithm are proposed. However, the computational complexity is higher due to using 2D-MUSIC algorithm. The DR-ESPRIT method is applied to distributed array radar is extended to the bistatic MIMO radar with distributed array in [17]. The high accuracy and non-ambiguous DOD and DOA estimation can be obtained by using unitary dual-resolution ESPRIT method. However, the DOD and DOA estimations are needed to pair, and the position information in the subarray is not fully utilized.

Therefore, in this paper, we link nested array to distributed subarray and propose the bistatic MIMO radar with distributed nested array to obtain a large virtual array aperture and high accuracy estimation. And a new corresponding joint DOD and DOA estimation algorithm, called automatically paired DR-ESPRIT based on the angle disambiguation algorithm by using the range information of targets is proposed. Furthermore, the performance of the algorithm is analyzed. The virtual extension of array aperture and high angle estimation accuracy can be achieved for the MIMO radar with automatic pairing and without increasing the number of antennas compared with traditional uniform linear MIMO array. Moreover, the proposed algorithm gives significant improvement in DOD and DOA estimation performance with Low computational complexity. The simulation results validate the theoretical algorithm and computational complexity.

The paper is organized as follows: section 1 is the introduction part; section 2 introduces proposed system model; section 3 introduces the automatically paired DR-ESPRIT based on the angle disambiguation algorithm by using the range information of targets; section 4 analyse the performance of the algorithm; section 5 verifies the superiority of our proposed strategy by simulation experiment; section 6 is the conclusion part.

## II. PROPOSED SYSTEM MODEL

As shown in Figure 1, a bistatic MIMO radar with distributed nested arrays system consists of  $N$ –element transmit array and  $M$ –element receive array. The transmit array is composed of two identical nested subarrays with  $M' = M/2$  sensors per subarray,  $d = \lambda/2d_{r1} = (M'/2 + 1)dd_{r2} = (M'/2)d$ . And the receive array is composed of two identical nested subarrays with  $N' = N/2$  sensors per subarray,  $d_{r1} = (N'/2 + 1)d$   $d_{r2} = (N'/2)d$ .  $\lambda$  is wavelength. In transmit array the inter-subarray spacing  $B_T$  and in receive array the inter-subarray spacing  $B_R$  are much larger

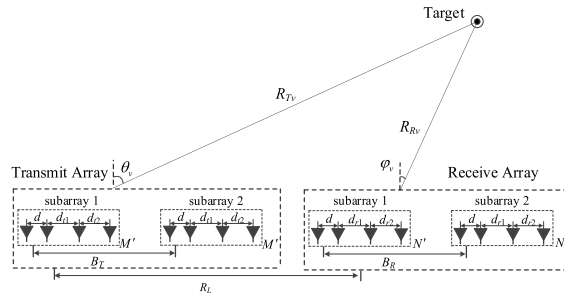


FIGURE 1. Array configuration of the bistatic MIMO radar with distributed nested arrays.

than half-wavelength. The transmitting antennas transmit  $M$  orthogonal waveforms with identical bandwidth and center frequency. In each receiver, the echoes are processed for scattering waveforms through  $V$  non-related far-field targets.  $R_L$  is baseline range between the bistatic arrays.  $R_{T_v}$  is range between the target  $v(v=1,2,\dots,V)$  and the transmit array and  $R_{R_v}$  is range between the target  $v$  and the receive array.  $R_B = R_{T_v} + R_{R_v}$  is baseline range between target  $v$  and the bistatic array. The transmit and receive angles corresponding to the target  $v$  are  $(\varphi_v)$ . Thus, in the  $q$ th ( $q = 1, 2, \dots, Q$ ) pulse, the output of the entire matched filters at the receive array can be written as

$$y_q(t) = A_T \text{diag}(\beta^q) A_R^H s(t) + n_q(t) \quad (1)$$

where  $A_T = [\mathbf{a}_T(\theta_1), \dots, \mathbf{a}_T(\theta_V)] \in \mathbb{C}^{M \times V}$  and  $A_R = [\mathbf{a}_R(\varphi_1), \dots, \mathbf{a}_R(\varphi_V)] \in \mathbb{C}^{N \times V}$  are the transmit steering matrix and the receive steering matrix, respectively. The  $\mathbf{a}_T(\theta_v) = [1, e^{-j2\pi B_T \sin \theta_v/\lambda}]^T \otimes [1, e^{-j2\pi d \sin \theta_v/\lambda}, e^{-j2\pi(M'-1)d \sin \theta_v/\lambda}]^T$  is the transmit steering vector of the  $v$ th target, and  $\mathbf{a}_R(\varphi_v) = [1, e^{-j2\pi B_R \sin \varphi_v/\lambda}]^T \otimes [1, e^{-j2\pi d \sin \varphi_v/\lambda}, e^{-j2\pi(M'-1)d \sin \varphi_v/\lambda}]^T$  is the receive steering vector of the  $v$ th target. “ $\otimes$ ” denotes the Kronecker product.  $\mathbf{s}(t) = [s_1(t), s_2(t), \dots, s_V(t)]^T$  denotes the signal vector.  $\beta^q = [\beta_1^q, \dots, \beta_V^q]^T$  denotes the dissipation coefficient vector of targets.  $n_q(t)$  denotes the white Gaussian noise vector. So the output of the receive array  $Y$  can be written as

$$Y = [y_1(t), \dots, y_q(t), \dots, y_Q(t)] \quad (2)$$

Thus, the covariance matrix of the received signal can be written as

$$R = E[YY^H] \quad (3)$$

The property of the Khatri-Rao (KR) product is used for vectorizing the covariance matrix  $R$

$$z = \text{vec}(R) = \{(A_R \odot A_T)^* \odot (A_R \odot A_T)\} \mathbf{h} + \sigma_n^2 \hat{\mathbf{I}} \quad (4)$$

where  $\text{vec}(\bullet)$  is vectorization function.  $\mathbf{h} = [\sigma_1^2, \dots, \sigma_V^2]^T$  is column vector of signal power,  $\sigma_v^2$ , ( $v = 1, 2, \dots, V$ ) is signal power of the  $v$ th target.  $\sigma_n^2$  is noise power.  $\hat{\mathbf{I}} = [e_1^T, \dots, e_{MN}^T]^T$ ,  $e_i$  is a vector of all zeros except a one at the center position.

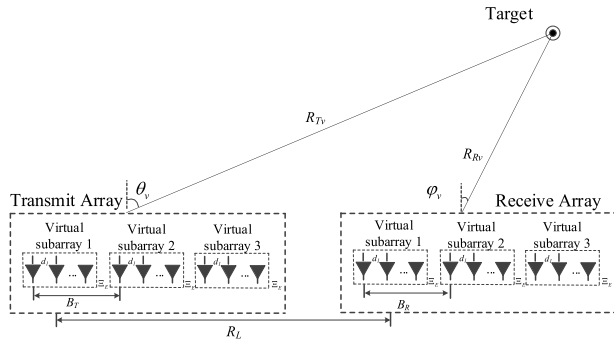


FIGURE 2. The bistatic MIMO radar with virtual arrays system.

$z$  is left-multiplied by the transformation matrix  $\Sigma$ , the new column vector  $\hat{z}$  can be obtained.

$$\hat{z} = \Sigma z = \{(A_R^* \odot A_R) \odot (A_T^* \odot A_T)\} h + \sigma_n^2 \Sigma \hat{I} \quad (5)$$

where  $\Sigma = I_M \otimes \Pi_s \otimes I_N$  is a  $MN \times MN$  dimensional matrix and the matrix  $\Pi_s \in \mathbb{C}^{MN \times MN}$  is given by

$$\Pi_s = \begin{bmatrix} \Gamma & & & \\ 0_{N \times 1} & \Gamma & & \\ \vdots & \vdots & \ddots & \\ 0_{N \times 1} & 0_{N \times 1} & \cdots & \Gamma \end{bmatrix} \quad (6)$$

where  $\Gamma$  is the  $M \times ((N - 1)M + 1)$  dimensional matrix in the following form

$$\Gamma = \begin{bmatrix} 1 & & & \\ 0_{1 \times M} & 1 & & \\ \vdots & \vdots & \ddots & \\ 0_{1 \times M} & 0_{1 \times M} & \cdots & 1 \end{bmatrix} \quad (7)$$

It is clear that the virtual array shown in figure 2 can be obtained from the above operation. The new output signal  $\bar{z}$  is obtained by eliminating the redundancy of the vector  $\hat{z}$ .

$$\bar{z} = \{\bar{A}_R \odot \bar{A}_T\} h + \sigma_n^2 \bar{e} \quad (8)$$

where  $\bar{A}_R = [\bar{a}_R(\varphi_1), \dots, \bar{a}_R(\varphi_V)]$ ,  $\bar{A}_T = [\bar{a}_T(\theta_1), \dots, \bar{a}_T(\theta_V)]$ ,  $\bar{e} = [0, \dots, 1, \dots, 0]^T$ . Let  $\Xi_E = (M^2 + 2)/2 + M'$ .  $\bar{a}_T(\theta_v)$  and  $\bar{a}_R(\varphi_v)$  can be expressed as:

$$\begin{aligned} \bar{a}_T(\theta_v) &= [1, e^{-j2\pi B_T \sin \theta_v / \lambda}, e^{-j2\pi (2B_T) \sin \theta_v / \lambda}]^T \\ &\quad \otimes [e^{-j2\pi d \sin \theta_v / \lambda}, \dots, e^{-j2\pi \Xi_E d \sin \theta_v / \lambda}]^T \\ \bar{a}_R(\varphi_v) &= [1, e^{-j2\pi B_R \sin \varphi_v / \lambda}, e^{-j2\pi (2B_R) \sin \varphi_v / \lambda}]^T \\ &\quad \otimes [e^{-j2\pi d \sin \varphi_v / \lambda}, \dots, e^{-j2\pi \Xi_E d \sin \varphi_v / \lambda}]^T \end{aligned} \quad (9)$$

The method of obtaining the new output signal  $\bar{z}$  by eliminating the redundancy of the vector  $\hat{z}$  is described below:

We remove repeated rows of  $(A_R^* \odot A_R)$  from virtual sensor positions at  $\{x_i - x_j, 1 \leq i, j \leq M\}$  and reorder them. A sorting array  $K_R$  is acquired and can be given by

$$K_R = \{k_1, k_2, \dots, k_{3\Xi_E}\} \quad (10)$$

Similarly, we remove repeated rows of  $(A_T^* \odot A_T)$  from virtual sensor positions at  $\{y_i - y_j, 1 \leq i, j \leq N\}$  and reorder them. A sorting array  $L_T$  is acquired and can be given by

$$L_T = \{l_1, l_2, \dots, l_{3\Xi_E}\} \quad (11)$$

Thus, we can construct an array containing  $G$  elements according to  $K_R$  and  $L_T$  in the following form

$$G_{(m-1) \times \Xi_E + n} = M^2 \times (k_m - 1) + l_n \quad (12)$$

where  $m = 1, 2, \dots, 3\Xi_E, n = 1, 2, \dots, 3\Xi_E$ .  $G$  also can be expressed as

$$G = \{g_1, g_2, \dots, g_{(3\Xi_E) \times (3\Xi_E)}\} \quad (13)$$

By extracting suitable rows using array  $G$  from  $\bar{z}$ , the new output signal  $\bar{Z}$  is obtained

$$\bar{z} = \bar{z}_{g_i}, i = 1, 2, \dots, (3\Xi_E) \times (3\Xi_E) \quad (14)$$

Because the new output signal is obtained by vectorization of the covariance matrix, the rank of the new output signal  $\bar{Z}$  is one. Thus we need to restore rank of it using 2-D spatial smoothing algorithm.

Let  $\Xi_H = (\Xi_E + 1)/2$ . Firstly, we construct a  $(3\Xi_H)^2 \times (3\Xi_E)^2$  selection matrix which is expressed as

$$\Delta_{m,n} = \Delta_{1n} \otimes \Delta_{2m} \quad (15)$$

where  $\Delta_{1n} = I_3 \otimes [0_{\Xi_H \times (\Xi_H - n)}, I_{\Xi_H} \otimes \Xi_H, 0_{\Xi_H \times (n-1)}]$ ,  $\Delta_{2m} = I_3 \otimes [0_{\Xi_H \times (\Xi_H - m)}, I_{\Xi_H} \otimes \Xi_H, 0_{\Xi_H \times (m-1)}]$ ,  $m = 1, 2, \dots, \Xi_H, n = 1, 2, \dots, \Xi_H$ .

We acquire the data covariance matrix  $R_\Theta$  which is given by

$$R_\Theta = \frac{1}{(\Xi_H)^2} \sum_{m=1}^{\Xi_H} \sum_{n=1}^{\Xi_H} (\Delta_{m,n} \bar{z})(\Delta_{m,n} \bar{z})^H \quad (16)$$

The steering vector matrix  $\hat{A} = [c(\theta_1, \varphi_1), \dots, c(\theta_V, \varphi_V)]$  is obtained by using 2D spatial smoothing. Where the  $v$ th column of the steering vector  $c(\theta_v, \varphi_v) = \hat{a}_R(\varphi_v) \otimes \hat{a}_T(\theta_v)$ ,

$$\begin{aligned} \hat{a}_T(\theta_v) &= [1, e^{-j2\pi B_T \sin \theta_v / \lambda}, e^{-j2\pi (2B_T) \sin \theta_v / \lambda}]^T \\ &\quad \otimes [e^{-j2\pi d \sin \theta_v / \lambda}, \dots, e^{-j2\pi \Xi_E d \sin \theta_v / \lambda}]^T \\ \hat{a}_R(\varphi_v) &= [1, e^{-j2\pi B_R \sin \varphi_v / \lambda}, e^{-j2\pi (2B_R) \sin \varphi_v / \lambda}]^T \\ &\quad \otimes [e^{-j2\pi d \sin \varphi_v / \lambda}, \dots, e^{-j2\pi \Xi_E d \sin \varphi_v / \lambda}]^T \end{aligned}$$

Perform eigen decomposition for  $R_\Theta$ , Let the signal subspace  $U_s$  be the matrix composed of the  $V$  eigenvectors corresponding to the largest  $V$  eigenvalues. It can be shown that  $U_s$  and  $\hat{A}$  span the same subspace. Thus, there is a non-singular matrix  $T$

$$U_s = \hat{A} T \quad (17)$$

### III. PROPOSED JOINT DOD AND DOA ESTIMATION

#### ALGORITHM METHOD

##### A. DOA COARSE ESTIMATION

Firstly, the first  $\Xi_H - 1$  and last  $\Xi_H - 1$  elements of each receive subarray in figure 2 are used to form subarray  $rc1$  and subarray  $rc2$ , respectively. There is the half wavelength rotational invariance relation between  $rc1$  and  $rc2$ . Thus, the rotation invariant relation equation (18) is given by

$$W_{rc2}\hat{A} = W_{rc1}\hat{A}\Theta_{rc} \quad (18)$$

where  $W_{rc1} = (I_3 \otimes [I_{(\Xi_H-1)}\mathbf{0}_{(\Xi_H-1)\times 1}]) \otimes I_{(3\Xi_H)}$  and  $W_{rc2} = (I_3 \otimes [0_{(\Xi_H-1)\times 1}I_{(\Xi_H-1)}]) \otimes I_{(3\Xi_H)}$  are selection matrix of  $rc1$  and  $rc2$ , respectively.  $\Theta_{rc} = \text{diag}\{v_{rc}^{(1)}, v_{rc}^{(2)}, \dots, v_{rc}^{(V)}\}$   $v_{rc}^{(v)} = e^{-j2xd \sin(\varphi_v)/\lambda}$ . Inserting (17) into (18), we can obtain

$$W_{rc2}\hat{A}T = W_{rc2}U_s = W_{rc1}U_s\Omega_{rc} \quad (19)$$

Obviously, where  $\Omega_c = T^{-1}\Theta_{rc}T$ . Let  $F = T^{-1}$ , then  $\Theta_{rc} = F^{-1}\Omega_{rc}F$ . Insert the signal subspace  $U_s$  into (19). The Equation (19) can be solved by least square method, we can obtain

$$\hat{\Omega}_{rc} = [W_{rc1}U_s]^+[W_{rc2}U_s] \quad (20)$$

where  $[\bullet]^+$  denotes the pseudo-inverse of the matrix. Perform eigen decomposition for  $\Omega_{rc}$ . And we can obtain its eigenvalues are  $\hat{v}_{rc}^{(v)}$ , ( $v = 1, 2, \dots, V$ )

$$\hat{\Theta}_{rc} = \hat{F}^{-1}\hat{\Omega}_{rc}\hat{F} \quad (21)$$

Thus, the low precision but non-ambiguous coarse direction-sine estimation of DOA  $\hat{\beta}_{rc}^{(v)}$  can be got.

$$\hat{\beta}_{rc}^{(v)} = \frac{\arg[\hat{v}_{rc}^{(v)}]}{2\pi d/\lambda} \quad (22)$$

where  $\hat{\Theta}_{rc} = \text{diag}\{\hat{v}_{rc}^{(v)}\}$ , ( $v = 1, 2, \dots, V$ ) is the  $V$  dimensional diagonal matrix.  $\arg[\hat{v}_{rc}^{(v)}]$  is phase of the  $v$  element of  $\hat{\Theta}_{rc}$ .

##### B. DOA AND DOD ACCURATE ESTIMATION

Firstly, the first two and last two subarrays of receive array in figure 2 are used to form subarray  $rf1$  and subarray  $rf2$ , respectively. There is  $B_R$  rotational invariance relation between  $rf1$  and  $rf2$ . The rotation invariant relation equation (23) is given by

$$W_{rf2}\hat{A} = W_{rf1}\hat{A}\Theta_{rf} \quad (23)$$

where  $W_{rf1} = [I_{(2\Xi_H)}\mathbf{0}_{(2\Xi_H)\times \Xi_H}] \otimes I_{(3\Xi_H)}$  and  $W_{rf2} = [0_{(2\Xi_H)\times \Xi_H} I_{(2\Xi_H)}] \otimes I_{(3\Xi_H)}$  are selection matrix of  $rf1$  and  $rf2$ , respectively.  $\Theta_{rf} = \text{diag}\{v_{rf}^{(1)}, v_{rf}^{(2)}, \dots, v_{rf}^{(V)}\}$ ,  $v_{rf}^{(v)} = e^{-j2\pi B_R \sin(\varphi_v)/\lambda}$ .

$U_s = \hat{A}T$ ,  $T$  is a non-singular matrix,  $F = T^{-1}$ . Thus we can estimate  $\hat{A}$  by  $\hat{F}$  and  $U_s$ .

$$\hat{A} = U_s\hat{F} \quad (24)$$

Thus the Equation (23) can then be written as

$$\hat{A}_{rf2} = \hat{A}_{rf1}\Theta_{rf} \quad (25)$$

where  $\hat{A}_{rf1} = W_{rf1}\hat{A}$ ,  $\hat{A}_{rf2} = W_{rf2}\hat{A}$ . Thus the estimation  $\hat{\Theta}_{rf}$  of  $\Theta_{rf}$  is given by

$$\hat{\Theta}_{rf} = \hat{A}_{rf2}\hat{A}_{rf1}^{-1} \quad (26)$$

It can be proved that  $\hat{\Theta}_{rf}$  and  $\Theta_{rf}$  are the diagonal matrix with the same elements and contain DOA information of the same target. Thus, The diagonal elements of  $\hat{\Theta}_{rf}$  can be expressed as

$$\hat{v}_{rf}^{(v)} = \frac{1}{(2\Xi_H) \times (3\Xi_H)} \sum_{i=1}^{6(\Xi_H)^2} \frac{(\hat{A}'_{rf2})^{iv}}{(\hat{A}'_{rf1})^{iv}} \quad (27)$$

where  $\hat{A}_{rf2}$  and  $(\hat{A}'_{rf1})^{iv}$  are the elements of the  $v$ th column of the matrix  $(\hat{A}'_{rf2})^{iv}$  and  $\hat{A}_{rf1}$ , respectively. Thus, the high accuracy but ambiguous fine direction-sine estimation of DOA  $\hat{\beta}_{rf}^{(v)}$  can be expressed as

$$\hat{\beta}_{rf}^{(v)} = \frac{\arg[\hat{v}_{rf}^{(v)}]}{2\pi B_R/\lambda} \quad (28)$$

We define a new steering vector  $\hat{A}' = [\hat{a}_T(\theta_1) \otimes \hat{a}_R(\varphi_1), \hat{a}_T(\theta_2) \otimes \hat{a}_R(\varphi_2), \dots, \hat{a}_T(\theta_V) \otimes \hat{a}_R(\varphi_V)]$ , obviously, there is a transformation matrix  $C$  so that  $\hat{A}' = C\hat{A}$ . And  $U'_s = \hat{A}'T = C\hat{A}'T$ .

Similar to DOA estimation, the first two and last two subarrays of transmit array in figure 2 are used to form subarray  $tf1$  and subarray  $tf2$ , respectively. There is  $B_T$  rotational invariance relationship between  $tf1$  and  $tf2$ . The rotation invariant relation equation (29) is given by

$$W_{tf2}\hat{A}' = W_{tf1}\hat{A}'\Phi_{tf} \quad (29)$$

where  $\Phi_{tf} = \text{diag}\{v_{tf}^{(1)}, v_{tf}^{(2)}, \dots, v_{tf}^{(V)}\}$ ,  $v_{tf}^{(v)} = e^{-j2\pi B_T \sin(\theta_v)/\lambda}$ .

The  $\hat{A}'$  can be estimated by  $\hat{F}$  and  $U'_s$ . The estimation  $\hat{A}'$  of  $\hat{A}'$  can be expressed as

$$\hat{A}' = U'_s\hat{F} \quad (30)$$

Thus the Equation (29) can then be written as

$$\hat{A}'_{tf2} = \hat{A}'_{tf1}\Phi_{tf} \quad (31)$$

where  $\hat{A}'_{tf1} = W_{tf1}\hat{A}'$ ,  $\hat{A}'_{tf2} = W_{tf2}\hat{A}'$ . Thus the estimation  $\hat{\Phi}_{tf}$  of  $\Phi_{tf}$  is given by

$$\hat{\Phi}_{tf} = \hat{A}'_{tf2}\hat{A}'_{tf1}^{-1} \quad (32)$$

It can be proved that  $\hat{\Phi}_{tf}$  and  $\Theta_{rc}$ ,  $\hat{\Phi}_{tf}$  are the diagonal matrix with the same elements and contain DOD and DOA

information of the same target. The diagonal elements of  $\hat{\Phi}_{tf}$  can be expressed as

$$\hat{v}_{tf}^{(v)} = \frac{1}{(2\Xi_H) \times (3\Xi_H)} \sum_{i=1}^{6(\Xi_H)^{\wedge 2}} \frac{(\hat{A}'_{tf2})^{iv}}{(\hat{A}'_{tf1})^{iv}} \quad (33)$$

where  $(\hat{A}'_{tf2})^{iv}$  and  $(\hat{A}'_{tf1})^{iv}$  are the elements of the  $v$ th column of the matrix  $\hat{A}'_{tf2}$  and  $\hat{A}'_{tf1}$ , respectively. Thus, the high accuracy but ambiguous fine direction-sine estimation of DOD  $\hat{\beta}'_{tf}^{(v)}$  can be expressed as

$$\hat{\beta}'_{tf}^{(v)} = \frac{\arg \left[ \hat{v}_{tf}^{(v)} \right]}{2\pi B_T / \lambda} \quad (34)$$

### C. DISAMBIGUATION OF THE ACCURATE ESTIMATION

From the description of the above algorithms, because the length of the baseline between the subarrays of the transmit array and the baseline between the subarrays of the receive array are much longer than half wavelength, the fine direction-sine estimation of DOA  $\hat{\beta}'_{rc}^{(v)}$  and DOD  $\hat{\beta}'_{rf}^{(v)}$  exist periodic ambiguity. The non-ambiguous direction-sine estimations  $\hat{\beta}_{rc}^{(v)}$ , ( $v = 1, 2, \dots, V$ ) can be serving as references to disambiguate the set of high accuracy but ambiguous estimations  $\hat{\beta}'_{rf}^{(v)}$ , ( $v = 1, 2, \dots, V$ ). The non-ambiguous and high accuracy sine estimations of DOA can be disambiguated by (35)

$$\beta_{rf}^{(v)} = \hat{\beta}'_{rf}^{(v)} + l_{rv}^{0(v)} \frac{\lambda}{B_R} \quad (35)$$

where  $l_{rv}^{0(v)} = \arg \min_{l_m^{(v)}} |\hat{\beta}'_{rc}^{(v)} - \hat{\beta}'_{rf}^{(v)} - l_m^{(v)} \lambda / B_R|$  donate the periodic fuzzy number of the fine direction-sine estimation of DOA  $\hat{\beta}'_{rf}^{(v)}$ , ( $v = 1, 2, \dots, V$ ). The  $l_{rv}^{0(v)}$  is integer, and its range of values is  $\lceil (-1 - \hat{\beta}'_{rf}^{(v)}) B_R / \lambda \rceil \leq l_{rv}^{(v)} \leq \lfloor (1 - \hat{\beta}'_{rf}^{(v)}) B_R / \lambda \rfloor$ . Thus, the non-ambiguous and high accuracy estimation of DOA  $\hat{\beta}_f^{(v)}$ , ( $v = 1, 2, \dots, V$ ) can be expressed as

$$\hat{\beta}_f^{(v)} = -\arcsin(\beta_{rf}^{(v)}) \quad (36)$$

From the diagram of array structure shown in figure 1, it can be seen that according to the geometric characteristics of the transmit angle  $\theta_v$ , the receive angle  $\varphi_v$ , the range sum between the target and the transceiver array  $R_B$ , and the range of the transceiver array  $R_L$ , the following relational equation [37] can be obtained.

$$\theta_v = \varphi_v + 2 \arctan \left( \frac{R_L \cos \varphi_v}{R_B + R_L \sin \varphi_v} \right) \quad (37)$$

Inserting  $\varphi_f^{(v)}$ , ( $v = 1, 2, \dots, V$ ) into (37), we can obtain the low precision but non-ambiguous estimation of DOD  $\hat{\theta}_{tc}^{(v)}$ , ( $v = 1, 2, \dots, V$ ) corresponding to the same target. Thus the sine estimations of DOD are. The  $\hat{\beta}_{tc}^{(v)} = \sin(\hat{\theta}_{tc}^{(v)}) = \sin \left( \varphi_f^{(v)} + 2 \arctan \left( R_L \cos \varphi_f^{(v)} / (R_B + R_L \sin \varphi_f^{(v)}) \right) \right)$  ( $v =$

$1, 2, \dots, V$ ) non-ambiguous and high accuracy sine estimations of DOD can be disambiguated by (38)

$$\beta_{tf}^{(v)} = \hat{\beta}'_{tf}^{(v)} + l_{vt}^{0(v)} \frac{\lambda}{B_T} \quad (38)$$

where  $l_{vt}^{0(v)} = \arg \min_{l_n^{(v)}} |\hat{\beta}'_{rc}^{(v)} - \hat{\beta}'_{tf}^{(v)} - l_n^{(v)} \lambda / B_T|$  donate the periodic fuzzy number of the fine direction-sine estimation of DOD  $\hat{\beta}'_{tf}^{(v)}$ , ( $v = 1, 2, \dots, V$ ). The  $l_{vt}^{(v)}$  is integer, and its range of values is  $\lceil (-1 - \hat{\beta}'_{tf}^{(v)}) B_T / \lambda \rceil \leq l_{vt}^{(v)} \leq \lfloor (1 - \hat{\beta}'_{tf}^{(v)}) B_T / \lambda \rfloor$ . Thus, The non-ambiguous and high accuracy estimation of DOD  $\theta_f^{(v)}$ , ( $v = 1, 2, \dots, V$ ) can be expressed as

$$\theta_f^{(v)} = -\arcsin(\beta_{tf}^{(v)}) \quad (39)$$

The major steps of the automatically paired dual-ESPRIT based on the angle disambiguation method by using the range information of targets for angle estimation in the bistatic MIMO radar with distributed nested arrays are summarized below.

**Step1.** Vectorize  $\mathbf{R}$  eliminate the redundancy and reorder them to obtain the new output signal  $\bar{\mathbf{Z}}$ .

**Step2.** Use 2-D spatial smoothing and perform eigendecomposition to obtain the signal subspace  $U_s$ .

**Step3.** Compute  $\hat{\Omega}_{rc} \hat{\Theta}_{rf}$  and  $\hat{\Phi}_{tf}$  as the solution to the rotational invariance equations in (18), (23) and (29), respectively.

**Step4.** Disambiguate the fine direction-sine estimations of DOA by (35), compute DOAs by (36).

Step5. Compute the DOD coarse estimations by (37).

**Step6.** Disambiguate the fine direction-sine estimations of DOD by (38), compute DODs by (39).

### IV. UNITS ERROR THRESHOLD ANALYSIS OF RANGE SUM BETWEEN TARGET AND TRANSCIEVER ARRAY

The coarse estimations of DOD are solved by using the range sum between target and the transceiver array  $R_B$ , and the range of the transceiver array  $R_L$  in proposed algorithm. The  $R_L$  can be obtained based on GPS or Beidou navigation, relatively accurate. However,  $R_B$  can only be obtained by using matched filtering. There are relative large error so that the ambiguity resolution will be invalid. In this section, the effect of error of  $R_B$  on angle estimation is analyzed and discussed.

According to the Equation (37), the error in calculating the coarse estimations of DOD is as follows

$$\left\{ \begin{array}{l} \Delta \hat{\theta}_{tc+}^{(v)} = \Delta \varphi_{rf}^{(v)} + 2 \arctan \left( \frac{R_L \cos(\varphi_v + \Delta \varphi_{rf}^{(v)})}{R_B - \Delta R + R_L \sin(\varphi_v + \Delta \varphi_{rf}^{(v)})} \right) \\ \quad - 2 \arctan \left( \frac{R_L \cos \varphi_v}{R_B + R_L \sin \varphi_v} \right) \\ \Delta \hat{\theta}_{tc-}^{(v)} = \Delta \varphi_{rf}^{(v)} + 2 \arctan \left( \frac{R_L \cos \varphi_v}{R_B + R_L \sin \varphi_v} \right) \\ \quad - 2 \arctan \left( \frac{R_L \cos(\varphi_v + \Delta \varphi_{rf}^{(v)})}{R_B - \Delta R + R_L \sin(\varphi_v + \Delta \varphi_{rf}^{(v)})} \right) \end{array} \right. \quad (40)$$

where  $\Delta R > 0$  is error of  $R_B$ .  $\Delta\hat{\theta}_{ic+}^{(v)} = \hat{\theta}_{ic}^{(v)} - \theta_v > 0$  and  $\Delta\hat{\theta}_{ic-}^{(v)} = \theta_v - \hat{\theta}_{ic}^{(v)} > 0$  are the coarse estimations error of DOD  $\hat{\theta}_{ic}^{(v)}$  when the range sum between target and the transceiver array exist error  $\Delta R$ .  $\Delta\varphi_f^{(v)} > 0$  are the fine estimations error of DOA.

According to the distributed array pattern, the maximum error angle of DOD coarse estimations are about the following when the DOD fine estimation can be solved correctly.

$$\begin{cases} \Delta\hat{\theta}_{\max+}^{(v)} \approx \arcsin(\sin \theta_v - \lambda/(2B_T)) - \theta_v \\ \Delta\hat{\theta}_{\max-}^{(v)} \approx \theta_v - \arcsin(\sin \theta_v - \lambda/(2B_T)) \end{cases} \quad (41)$$

So, when  $\Delta\hat{\theta}_{ic+}^{(v)} < \Delta\hat{\theta}_{\max+}^{(v)} \cup \Delta\hat{\theta}_{ic-}^{(v)} < \Delta\hat{\theta}_{\max-}^{(v)}$ , the DOD fine estimation can be solved correctly. Inserting (40) into (42), then the maximum error angle of DOD coarse estimations are obtained by

$$\begin{cases} \Delta\hat{\theta}_{\max+}^{(v)} = \Delta\varphi_{rf}^{(v)} - 2 \arctan\left(\frac{R_L \cos \varphi_v}{R_B + R_L \sin \varphi_v}\right) + 2 \arctan\left(\frac{R_L \cos(\varphi_v + \Delta\varphi_{rf}^{(v)})}{R_B - \Delta R_{\max+}^{(v)} + R_L \sin(\varphi_v + \Delta\varphi_{rf}^{(v)})}\right) \\ \Delta\hat{\theta}_{\max-}^{(v)} = \Delta\varphi_{rf}^{(v)} + 2 \arctan\left(\frac{R_L \cos \varphi_v}{R_B + R_L \sin \varphi_v}\right) - 2 \arctan\left(\frac{R_L \cos(\varphi_v + \Delta\varphi_{rf}^{(v)})}{R_B - \Delta R_{\max-}^{(v)} + R_L \sin(\varphi_v + \Delta\varphi_{rf}^{(v)})}\right) \end{cases} \quad (42)$$

where  $\Delta R_{\max+}^{(v)}$  and  $\Delta R_{\max-}^{(v)}$  are the maximum error of  $R_B$  when  $\hat{\theta}_{ic}^{(v)} > \theta_v$  and  $\hat{\theta}_{ic}^{(v)} < \theta_v$ .

Therefore, for all  $V$  targets, the approximate threshold for the error  $\Delta R_{\max}$  of the range sum between target and the transceiver array  $R_B$  can be expressed as

$$\Delta R_{\max} = \min_{v=1, \dots, V} \left\{ \min \left\{ \Delta R_{\max+}^{(v)}, \Delta R_{\max-}^{(v)} \right\} \right\} \quad (43)$$

If the effect of  $\Delta\varphi_{rf}^{(v)}$  is ignored, The Equation (42) is also denoted by

$$\begin{cases} \Delta\hat{\theta}_{\max+}^{(v)} = 2 \arctan\left(\frac{R_L \cos \varphi_v}{R_B - \Delta R_{\max+}^{(v)} + R_L \sin \varphi_v}\right) - 2 \arctan\left(\frac{R_L \cos \varphi_v}{R_B + R_L \sin \varphi_v}\right) \\ \Delta\hat{\theta}_{\max-}^{(v)} = 2 \arctan\left(\frac{R_L \cos \varphi_v}{R_B + R_L \sin \varphi_v}\right) - 2 \arctan\left(\frac{R_L \cos \varphi_v}{R_B - \Delta R_{\max-}^{(v)} + R_L \sin \varphi_v}\right) \end{cases} \quad (44)$$

Therefore, for all  $V$  targets, the approximate threshold for the error lax of the range sum between target and the transceiver array  $R_B$  can be expressed as

$$\widehat{\Delta R}_{\max} = \min_{v=1, \dots, V} \left\{ \min \left\{ \widehat{\Delta R}_{\max+}^{(v)}, \widehat{\Delta R}_{\max-}^{(v)} \right\} \right\} \quad (45)$$

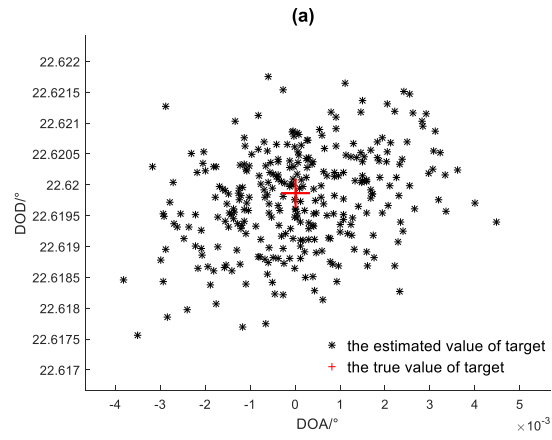
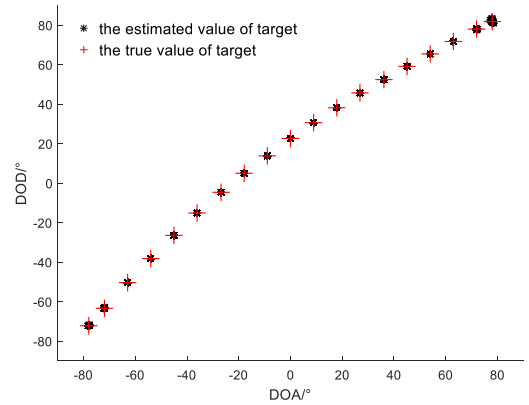


FIGURE 3. The joint DOD and DOA estimation results of nineteen targets. (a) Estimation results. (b) Drawing of partial enlargement.

### V. DISCUSSION

In this section, we use numerical examples to show the superiority of our proposed strategy. We provide several sets of simulation results to demonstrate the performance. In all the simulation examples below, SNR is defined as

$$SNR = 10 \log_{10} \frac{E[x(t)^2]}{E[n(t)^2]}$$

The root mean square error (RMSE) is defined as

$$RMSE = \sqrt{\frac{1}{K} \frac{1}{V} \sum_{j=1}^K \sum_{i=1}^V |\hat{\theta}_i - \theta_i|^2}$$

where  $K$  is the number of Monte Carlo trials. where  $\theta_i$  is the true value of target, and  $\hat{\theta}_i$  is estimated value of  $\theta_i$ .

We consider the bistatic MIMO radar with distributed nested arrays system with  $M = 8, N = 8; M_1 = 2, N_1 = 2$ . Both the long baseline in the transmit array and in the receive array are  $B_T = B_R = 25\lambda$ . Assume that SNR = 10dB, the number of snapshots is  $L = 100$ , the range sum between target and the transceiver array is  $R_B = 20\text{km}$ , the range of the transceiver array  $R_L = 100\text{km}$ . The signals are far-field narrowband signals. Figure 3 depicts the angle estimation results of nineteen targets with 300 Monte Carlo trials. As we can see in the figure 3, the DODs and DOAs of all the nineteen targets

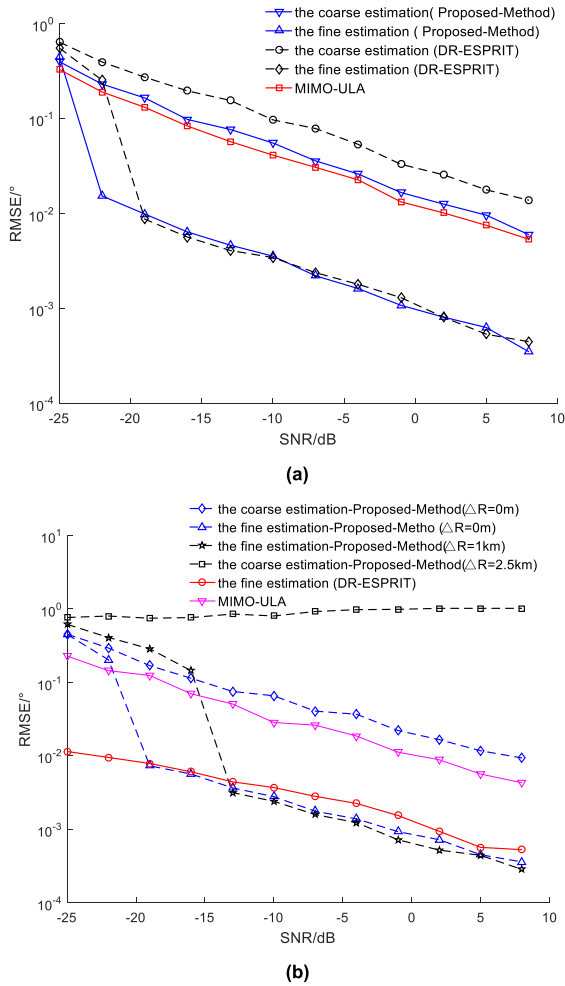


FIGURE 4. The RMSE of angle estimation versus SNR. (a) The RMSE of DOA estimation versus SNR. (b) The RMSE of DOD estimation versus SNR.

are correctly paired and well localized, and there is not too much diffusion, which reflects the robustness of the algorithm in angle estimation. the long baseline and short baseline in the transceiver arrays are virtually extended simultaneously so that the maximum number of the identifiable targets is 30 in theory.

The angle estimation RMSE of the proposed algorithm and the methods of [8] and [18] versus SNR are shown in Figure 4. From Figures 4, we can see that the performances of the proposed algorithm with distributed nested arrays are much better than MIMO-ULA of [8] and DR-ESPRIT with sparse array of [18]. Because the long baseline and short baseline in the transceiver arrays are virtually extended simultaneously. The proposed algorithm gives significant improvement in DOD and DOA estimation performance. Moreover, an upper limit for the gain of accuracy is existed in the proposed algorithm and the methods of [18]. As the SNR decrease, the error of the coarse estimations increase. The probability of the disambiguation becomes decreasing. The upper limit of the proposed algorithm is lower than the methods of [18]. Furthermore, as can be seen from figure 4(b), when the  $R_B$

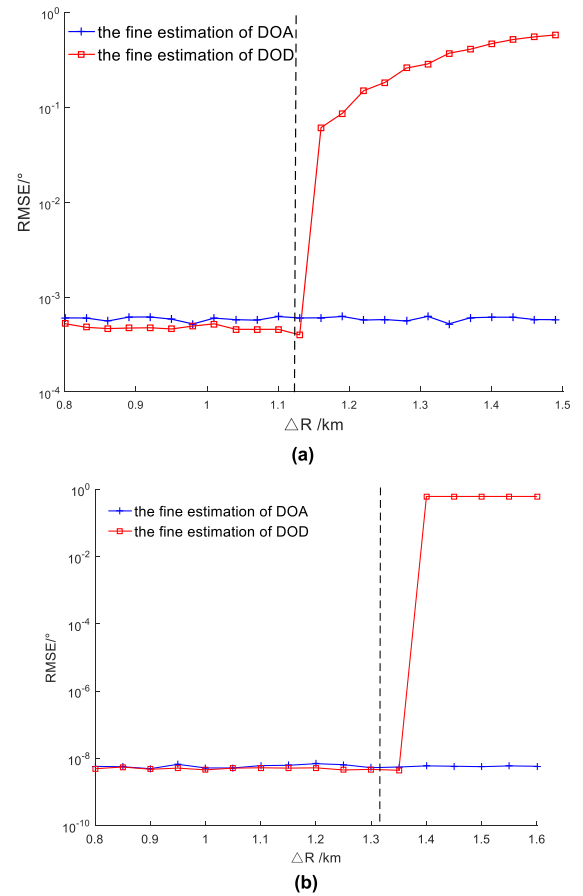


FIGURE 5. The RMSE of angle estimation versus the error. (a) SNR = 0dB. (b) SNR = 50dB.

exists measurement error  $\Delta R = 1$ km, the algorithm can still effectively disambiguate the fine estimations of DOD, but the signal-to-noise ratio threshold obviously increases. When the  $R_B$  exists measurement error  $\Delta R = 2.5$ km too large, No matter how high the SNR is, the algorithm can not still effectively disambiguate the fine estimations of DOD.

Figures 5(a) show the RMSE of angle estimation versus the error  $\Delta R$  of the range sum between target and the transceiver array when SNR = 0dB (error of DOA estimations are existent). And Figures 5(b) show the RMSE of angle estimation versus the error  $\Delta R$  of the range sum between target and the transceiver array when SNR = 50dB (error of DOA estimations are non-existent). From the two figures, we can see that the error of the range sum between target and the transceiver array has obvious threshold effect. When the error of the range sum between target and the transceiver array are  $\Delta R > 1.13$  km (error of DOA estimations are existent) and  $\Delta \hat{R} > 1.35$  km (error of DOA estimations are non-existent), respectively, the algorithm can not effectively disambiguate the fine estimations of DOD so that the RMSE of DOD estimations are deteriorating rapidly. According to the simulation experiment conditions set above, we can obtain the approximate threshold for the error  $\Delta R_{\max}$  and  $\Delta \hat{R}_{\max}$  of

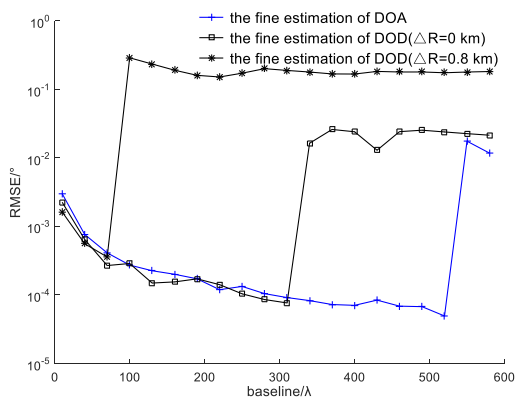


FIGURE 6. The angle estimation RMSE versus baseline.

the range sum between target and the transceiver array are  $\Delta R_{\max} = 1.1123\text{km}$  and  $\Delta R_{\max} = 1.316\text{km}$  by equation (43) and (45), respectively.

The angle estimation RMSE of the proposed algorithm versus SNR is shown in Figure 6. From Figures 6, we can see that the angle estimation accuracy of the proposed algorithm is proportional to the long baseline. However, the threshold for the gain of accuracy is existed in the proposed algorithm. For the RMSE of DOD, as the error of the range sum between target and the transceiver array increase, the threshold of the baseline decrease.

VI. CONCLUSION

In this paper, we present a novel array configuration, called bistatic MIMO radar with distributed nested array, for joint angle estimation of multiple targets in bistatic MIMO radar. The DOD and DOA estimation algorithm, called automatically paired DR-ESPRIT based on the angle disambiguation algorithm by using the range information of targets is proposed. By designing distributed nested array and using Khatri-Rao product processing, the long baseline and short baseline in the transceiver arrays are virtually extended simultaneously without increasing hardware complexity. Some examples showing typical results were presented. It is found that the angle measurement performance and target resolution of the algorithm are further improved. Furthermore, the proposed algorithm doesn't requires no pair matching.

REFERENCES

[1] E. Fishler, A. Haimovich, R. Blum, D. Chizhik, L. Cimini, and R. Valenzuela, "MIMO radar: An idea whose time has come," in *Proc. IEEE Radar Conf.*, Apr. 2004, pp. 71–78.

[2] S. Zhuang and X. Zhu, "Improved design of unimodular waveforms for MIMO radar," *Multidimensional Syst. Signal Process.*, vol. 24, no. 3, pp. 447–456, 2013.

[3] M. Jin, G. Liao, and J. Li, "Target localisation for distributed multiple-input multiple-output radar and its performance analysis," *IET Radar Sonar Navigat.*, vol. 5, no. 1, pp. 83–91, Jan. 2011.

[4] L. Li, "Cramer-Rao bound for parameter estimation in narrowband bistatic MIMO radar," *Appl. Mech. Mater.*, vols. 556–562, pp. 5034–5037, May 2014.

[5] X. Zhang and D. Xu, "Angle estimation in MIMO radar using reduced-dimension capon," *Electron. Lett.*, vol. 46, no. 12, pp. 860–861, Jun. 2010.

[6] X. F. Zhang, L. Y. Xu, L. Xu, and D. Z. Xu, "Direction of departure (DOD) and direction of arrival (DOA) estimation in MIMO radar with reduced-dimension MUSIC," *IEEE Commun. Lett.*, vol. 14, no. 12, pp. 1161–1163, Dec. 2010.

[7] C. Duofang, C. Baixiao, and Q. Guodong, "Angle estimation using ESPRIT in MIMO radar," *Electron. Lett.*, vol. 44, no. 12, pp. 770–771, Jun. 2008.

[8] C. Jinli, G. Hong, and S. Weimin, "Angle estimation using ESPRIT without pairing in MIMO radar," *Electron. Lett.*, vol. 44, no. 24, pp. 1422–1423, Nov. 2008.

[9] M. L. Bencheikh and Y. Wang, "Joint DOD-DOA estimation using combined ESPRIT-MUSIC approach in MIMO radar," *Electron. Lett.*, vol. 46, no. 15, pp. 1081–1083, Jul. 2010.

[10] C. Y. Chen and P. P. Vaidyanathan, "Minimum redundancy MIMO radars," in *Proc. IEEE Int. Symp. Circuits Syst.*, May 2008, pp. 45–48.

[11] B. Yao, W. Wang, and Q. Yin, "DOD and DOA estimation in bistatic non-uniform multiple-input multiple-output radar systems," *IEEE Commun. Lett.*, vol. 16, no. 11, pp. 1796–1799, Nov. 2012.

[12] P. Pal and P. P. Vaidyanathan, "Coprime sampling and the music algorithm," in *Proc. IEEE Digit. Signal Process. Workshop IEEE Signal Process. Educ. Workshop*, Jan. 2011, pp. 289–294.

[13] H. Qi, H. Jiang, and S. Yao, "Joint multi-target DOD and DOA estimation in bistatic MIMO radar exploiting 2-level nested arrays," in *Proc. Int. Conf. Radar Syst. (Radar)*, Belfast, U.K., Oct. 2017, pp. 1–4.

[14] G. H. Chen, "High accuracy 2-D angle estimation using distributed coherent arrays," *J. Electron. Inf. Technol.*, vol. 34, no. 11, pp. 2621–2627, 2012.

[15] X. Yang, B. Chen, and Y. Chen, "An eigenstructure-based 2D DOA estimation method using dual-size spatial invariance array," *Sci. China, Inf. Sci.*, vol. 54, no. 1, pp. 163–171, 2011.

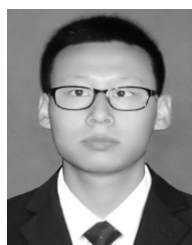
[16] C. Zhang and Y. Pang, "Sparse array angle estimation using reduced-dimension ESPRIT-MUSIC in MIMO radar," *Sci. World J.*, vol. 5, 2013, Art. no. 784267.

[17] G. Zheng and B. Chen, "Unitary dual-resolution ESPRIT for joint DOD and DOA estimation in bistatic MIMO radar," *Multidimensional Syst. Signal Process.*, vol. 26, no. 1, pp. 159–178, 2015.

[18] M. C. Jackson, "The geometry of bistatic radar systems," *IEE Proc. F Commun., Radar Signal Process.*, vol. 133, no. 7, pp. 604–612, Dec. 1986.



**YANPING LIAO** was born in Changchun City, Jilin Province, China, in 1980. From 1999 to 2007, she received the B.S. degree and Ph.D. degrees in information and communication engineering from Harbin Engineering University. Since 2010, she has been an Associate Professor with the Department of Information and Communication Engineering, Harbin Engineering University.



**RUIGANG ZHAO** was born in Baoji City, Shaanxi Province, China, in 1994. From 2012 to 2016, he received the B.S. degrees in information countermeasure technology from Harbin Engineering University. Since 2016, he has been working toward the master's degree in information and communication engineering at Harbin Engineering University, Department of Information and Communication Engineering.



**LIPENG GAO** was born in Harbin City, Helongjiang Province, China, in 1972. From 1996 to 2006, he received the B.S., M.S., and Ph.D. degrees in information and communication engineering from Harbin Engineering University. Since 2010, he has been a Professor with the Department of Information and Communication Engineering, Harbin Engineering University.